An Efficient Implementation of Lattice Staggered Multicarrier Faster-than-Nyquist Signaling

Siming Peng, Aijun Liu, Xinhai Tong, and Giulio Colavolpe, *Senior Member, IEEE*

***Abstract*—In this letter, we investigate the lattice staggered multicarrier faster-than-Nyquist (MFTN) signaling. Specifically, we consider the time-frequency packing and optimal hexagonal lattice over additive white Gaussian noise channels. Firstly, an efficient implementation of the lattice staggered MFTN based on the fast Fourier transform algorithm is proposed, and we show that the modulation and demodulation complexity could be substantially reduced. Furthermore, we consider, at the receiver, a low-complexity symbol-by-symbol detector. Our practical spectral efficiency and bit-error-rate performance investigation demonstrates that the MFTN with optimal hexagonal lattice outperforms the conventional rectangular lattice.**

***Index Terms*—Multicarrier communication, faster-than-Nyquist, time-frequency packing, spectral efficiency, lattice staggering, fast Fourier transform.**

I. Introduction

MULTICARRIER faster-than-Nyquist (MFTN) signaling, also known as time-frequency packing signaling (TFPS), is a spectrally efficient linear transmission scheme for future communication systems [1]–[3]. By both time packing the adjacent symbols and reducing the frequency spacing of the adjacent subcarriers with respect to the Nyquist signaling systems, the information symbols of MFTN can be transmitted by employing less time and bandwidth resources. However, since MFTN violates the Nyquist criterion, interpulse interference (IPI) is thus introduced intentionally. It is known that for multicarrier transmissions, the system performance will be mainly determined by two factors: 1) the time-frequency localization of the base pulse and 2) the distance between adjacent symbols in the time-frequency plane. Hence, the hexagonal lattice is considered to be a better choice than the conventional rectangular lattice when a simple linear receiver is employed [4]. As shown in [5]–[6], the minimum Euclidean distance could be improved for the lattice staggered MFTN with respect to rectangular MFTN. This is expected to be true even when the target is the optimization of the spectral efficiency, as in the case of TFPS.

On the other hand, the efficient implementation of lattice staggered MFTN is also a major challenge. Although the discrete Fourier transform (DFT)-based implementation has been widely investigated for conventional Nyquist multicarrier systems [7]–[8], similar works are still not well established for MFTN signaling system. In [9], the time-packed MFTN signals were projected to a series of orthogonal bases so as the MFTN signals could be equivalently obtained by the Nyquist signals. However, the projection operation will bring additional complexity especially when an accurate approximation is considered. Furthermore, an efficient implementation of the MFTN based on overcomplete Gabor frames has been proposed in [10], but it may not suitable for general time-frequency packing systems. On the other hand, it was shown in [11] that the frequency or time-frequency packing may obtain a better system performance than time-packing alone under the same conditions. Hence, since the subcarriers in frequency packed MFTN signaling system are not orthogonal to each other anymore, the efficient implementation is still a problem.

In this letter, we investigate the lattice staggered MFTN signaling system. Different from previous works [6], [10], we present an efficient implementation of the lattice staggered MFTN when frequency packing is involved. In this regard, we show that the MFTN signaling system could be efficiently implemented by exploiting multiple parallel IFFT/FFT blocks and combining the IFFT/FFT outputs with proper phase rotations before stacking/summation operation. Moreover, we consider a low complexity symbol-by-symbol receiver. The practical spectral efficiency and error performance investigation over AWGN channels validates that the lattice staggered MFTN permits further improvements of the system performance with respect to conventional rectangular MFTN signaling scheme.

II. System Model

Considering an MFTN signaling system based on the optimal hexagonal lattice with K subcarriers, the complex envelope of the transmitted signal can be expressed as

$$\begin{aligned} s(t) &= \sum_l \sum_k a_{l,k} g(t - l_{(k)}\tau T) e^{j2\pi k\upsilon F(t - l_{(k)}\tau T)} \\ &= \sum_l \sum_k \Big[a_{l,2k} g(t - l\tau T) e^{j2\pi 2k\upsilon F(t - l\tau T)} + \\ &\quad a_{l,2k+1} g(t - (l+\tfrac{1}{2})\tau T) e^{j2\pi (2k+1)\upsilon F(t - (l+\frac{1}{2})\tau T)} \Big] \end{aligned} \tag{1}$$

where $\{a_{l,k}\}$ are independent and uniformly distributed (i.u.d) information symbols with l being the time index and k the subcarrier index, respectively. $g(t)$ is the unit-energy shaping pulse (in the following, we will assume that pulse $g(t)$ is a Nyquist pulse, i.e., $\int_{-\infty}^{\infty} g(t - mT) g^*(t - nT) dt = 0, m \neq n$, where T is the Nyquist time interval. In the numerical results, we will relax this constraint by also considering different pulses). $l_{(k)} = l + \frac{1}{2} \bmod (k, 2)$, $\bmod (a, b)$ denotes a modulo b. F is the minimum orthogonal subcarrier spacing, and

This work is supported by the National Natural Science Foundation of China (grant no 61671476).

S. Peng, A. Liu, X. Tong are with the College of Communications Engineering, PLA University of Science and Technology, Nanjing 210007, China (e-mail: lgdxpsm@gmail.com, liuaj.cn@163.com, tongxinhai2012@163.com).

G. Colavolpe is with Università di Parma, Dipartmento di Ingegneria e Architettura, Parco Area delle Scienze, 181A, 43124 Parma, Italy (email: giulio.colavolpe@unipr.it).

This article has been accepted for publication in a future issue of this journal, but has not been fully edited. Content may change prior to final publication. Citation information: DOI 10.1109/LCOMM.2017.2774260, IEEE Communications Letters

$\tau, \upsilon \in (0,1]$ are the time and frequency packing factor, respectively.

Under the assumption of transmission over an AWGN channel, the continuous-time received signal is

$$r(t) = s(t) + w(t) \tag{2}$$

where $w(t)$ is the white noise with power spectral density N_0.

The observed sample after matched filtering at discrete-time $l\tau T$ for the k-th subcarrier is

$$r_{l,k} = \int_{-\infty}^{\infty} r(t) g^*(t - l_{(k)}\tau T) e^{-j2\pi k\upsilon F(t - l_{(k)}\tau T)} dt \tag{3}$$

By substituting (1) and (2) into (3), we obtain

$$r_{l,k} = a_{l,k} + \sum_{(m',n')\neq(0,0)} a_{m',n'} \psi_{m',n'} + n_{l,k} \tag{4}$$

where we defined $m' = l_{(k)} - m_{(n)}, n' = k - n$, and $\psi_{m',n'} = A_g(m'\tau T, n'\upsilon F) e^{j2\pi k m'\upsilon\tau}$, $A_g(\tau,\upsilon) = \int_{-\infty}^{\infty} g(t-\tau) g^*(t) e^{-j2\pi\upsilon t} dt$ being the *ambiguity function* which characterizes the interference among adjacent symbols, and the noise sample is $n_{l,k} = \int_{-\infty}^{\infty} w(t) g^*(t - l_{(k)}\tau T) e^{-j2\pi k\upsilon F(t - l_{(k)}\tau T)} dt$.

As in [2], [12], we model the contribution of ISI and ICI in (4) as a zero-mean Gaussian process with power spectral density E_I independent of the additive noise. With the above assumption, the signal model assumed by the receiver, i.e., the so-called auxiliary channel model, becomes

$$r_{l,k} = a_{l,k} + \eta_{l,k} \tag{5}$$

where $\eta_{l,k}$ is the equivalent interference noise with variance $N_I = N_0 + E_I$, and

$$E_I = \sum_{(m',n')\neq(0,0)} \left| A_g(m'\tau T, n'\upsilon F) \right|^2. \tag{6}$$

We remark that the simplified channel model (5) is only used by the receiver, and the actual channel interference is still generated as (4).

III. Efficient Implementation

A. Efficient Implementation of Modulator

Assume that the frequency packing factor is a rational number, i.e., $\upsilon = b/c$ and $b < c, b, c \in \mathbb{N}_+$ and denote by T_c the sampling interval. We will also assume that T is a multiple of T_c (and we will define $N = T/T_c$) and that the sampling rate used for discretizing all signals is $1/T_c = KF$. Moreover, for a given generic signal $x(t)$, we define $x[n] = x(nT_c)$ and the pulse $g[n]$ has finite (possibly very long) support $[-L_g/2, L_g/2]$, where L_g is the length of shaping pulse. Hence, the samples of the transmitted signal (1) can be expressed as

$$\begin{aligned} s[n] &= \sum_l \sum_k a_{l,k} g[n - l_{(k)}\tau N] e^{j2\pi(n - l_{(k)}\tau N)\upsilon k/K} \\ &= \sum_l \sum_{k=0}^{K/2-1} \Big(a_{l,2k} e^{j2\pi(n - l\tau N)\upsilon 2k/K} g[n - l\tau N] + \\ &\quad a_{l,2k+1} e^{j2\pi(n - (l+\frac{1}{2})\tau N)(2k+1)\frac{\upsilon}{K}} g[n - (l+\tfrac{1}{2})\tau N] \Big) \\ &= s^{(1)}[n] + s^{(2)}[n]\,. \end{aligned} \tag{7}$$

According to [13], for the l-th symbol period, $s^{(1)}[n]$ can be expressed as

$$\begin{aligned} s^{(1)}[n] &= \sum_l \sum_{k=0}^{K/2-1} a_{l,2k} e^{j2\pi(n - l\tau N)\upsilon 2k/K} g[n - l\tau N] \\ &= \sum_{i=l}^{l+L-1} \dot{s}_i[n - i\tau N], n \in [l\tau N, (l+1)\tau N - 1] \end{aligned} \tag{8}$$

where $L = \lceil L_g/(\tau N) \rceil$ is the number of overlapped transmit pulses. The partial transmit signals $\dot{s}_i[n]$ are obtained by windowing the transmit symbols $\{a_{l,2k}\}$, i.e.,

$$\begin{aligned} \dot{s}_i[n] &= \sum_{k=0}^{K/2-1} a_{i,2k} e^{j2\pi n 2bk/cK} g[n] \\ &= \sum_{\dot{k}=0}^{cK/2-1} \dot{a}_{i,2\dot{k}} e^{j2\pi n\dot{k}/(cK/2)} g[n] \end{aligned} \tag{9}$$

where $\{\dot{a}_{i,2\dot{k}}\}$ is a $cK/2$-dimensional vector with the elements taking the values of either the input symbols $a_{i,2k}$ or zeros as

$$\dot{a}_{i,2\dot{k}} = \begin{cases} a_{i,2\dot{k}/b}, & \text{if } 2\dot{k} \bmod b = 0 \text{ and } 2\dot{k}/b \leq K-1 \\ 0, & \text{otherwise.} \end{cases} \tag{10}$$

Defining $\dot{k} = cp + d$, then, (9) can be further expressed as

$$\begin{aligned} \dot{s}_i[n] &= \sum_{d=0}^{c-1} \sum_{p=0}^{K/2-1} \dot{a}_{i,2(cp+d)} e^{j2\pi n \frac{cp+d}{cK/2}} g[n] \\ &= \sum_{d=0}^{c-1} e^{j2\pi n \frac{d}{cK/2}} \underbrace{\sum_{p=0}^{K/2-1} \dot{a}_{i,2(cp+d)} e^{j2\pi n \frac{p}{K/2}}}_{IFFT} g[n]. \end{aligned} \tag{11}$$

Similarly to the above derivations, for the l-th symbol period, $s^{(2)}[n]$ can be expressed as

$$s^{(2)}[n] = \sum_{i=l}^{l+L-1} \ddot{s}_i[n - i\tau N] \tag{12}$$

where $n \in [l\tau N + \tau N/2, (l+1)\tau N + \tau N/2 - 1]$, and

$$\begin{aligned} \ddot{s}_i[n] &= \sum_{k=0}^{K/2-1} a_{i,2k+1} e^{j2\pi n b(2k+1)/cK} g[n] \\ &\overset{(a)}{=} e^{j2\pi n b/cK} \sum_{\ddot{k}=0}^{cK/2-1} \ddot{a}_{i,2\ddot{k}+1} e^{j2\pi n \frac{\ddot{k}}{cK/2}} g[n] \\ &\overset{(b)}{=} e^{j2\pi n b/cK} \sum_{d=0}^{c-1} \sum_{p=0}^{K/2-1} \ddot{a}_{i,2(cp+d)+1} e^{j2\pi n \frac{cp+d}{cK/2}} g[n] \\ &= \sum_{d=0}^{c-1} e^{j2\pi n \frac{d+b/2}{cK/2}} \underbrace{\sum_{p=0}^{K/2-1} \ddot{a}_{i,2(cp+d)+1} e^{j2\pi n \frac{p}{K/2}}}_{IFFT} g[n] \end{aligned} \tag{13}$$

where in steps (a) and (b) of (13) we used the same mapping operations as in (10) and (11).

From (8)-(13), we can see that as general pulse-shaped multicarrier transmission systems, the lattice staggered MFTN can be implemented by two adjacent rectangular sub-lattices, and for each of them, it can be efficiently implemented by means of c parallel $K/2$-point IFFT blocks whose outputs are combined through proper phase rotations before stacking them to the length of the shaping pulse. The block diagram of the modulator is shown in Fig. 1(a).

This article has been accepted for publication in a future issue of this journal, but has not been fully edited. Content may change prior to final publication. Citation information: DOI 10.1109/LCOMM.2017.2774260, IEEE Communications Letters

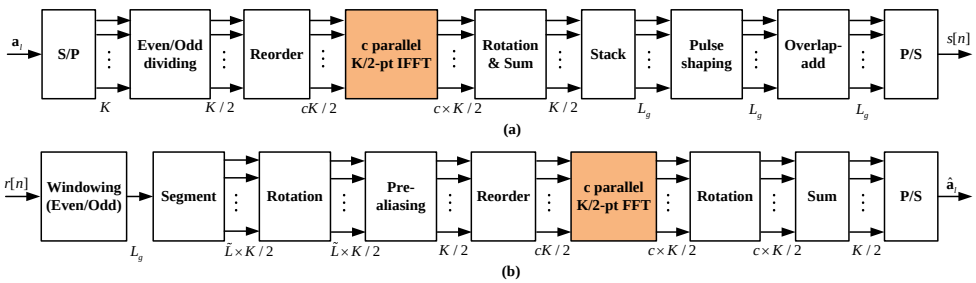

Fig. 1. Block diagram of the efficient implementation of lattice staggered MFTN signaling system. (a) Modulator, (b) demodulator.

B. Efficient Implementation of Demodulator

At the receiver, for the even signal component, the received signal samples $\{r[n]\}$ are demodulated according to

$$\begin{aligned}\hat{a}_{l,2k} &= \sum_{n=l\tau N}^{l\tau N+L_g-1} r[n]g^*[n-l\tau N]e^{-j2\pi 2k(n-l\tau N)\frac{\upsilon}{K}} \\ &= \sum_{n=0}^{L_g-1} \tilde{r}_l[n]e^{-j2\pi 2kn\frac{\upsilon}{K}}\end{aligned} \tag{14}$$

where $\tilde{r}_l[n] = r[n+l\tau N]g^*[n]$. Then, (14) can be further expressed as

$$\begin{aligned}\hat{a}_{l,2k} &= \sum_{n=0}^{K/2-1}\sum_{\tilde{i}=0}^{\tilde{L}-1} \tilde{r}_l[n+\tilde{i}K/2]e^{-\frac{j2\pi 2bk(n+\tilde{i}K/2)}{cK}} \\ &= \sum_{\dot{n}=0}^{cK/2-1}\sum_{\tilde{i}=0}^{\tilde{L}-1} e^{-\frac{j2\pi bk\tilde{i}}{c}}\dot{r}_l[\dot{n}+\tilde{i}K/2]e^{-\frac{j2\pi \dot{n}k}{cK/2}}\end{aligned} \tag{15}$$

where $\tilde{L} = \lceil L_g/(K/2)\rceil$ is the number of segments for the matched-filtered data block before summation operation, and we used the mapping

$$\dot{r}_l[\dot{n}+\tilde{i}K/2] = \begin{cases} \tilde{r}_l[\dot{n}/b+\tilde{i}K/2], \text{if } \dot{n} \bmod b = 0 \\ 0, \qquad\qquad \text{otherwise}. \end{cases} \tag{16}$$

Taking $\dot{n} = cp+d$ and with a small abuse of notation, (15) can be further expressed as

$$\begin{aligned}\hat{a}_{l,2k} &= \sum_{d=0}^{c-1}\sum_{p=0}^{K/2-1}\sum_{\tilde{i}=0}^{\tilde{L}-1} e^{-j2\pi bk\tilde{i}/c}\dot{r}_l[cp+d]e^{\frac{-j2\pi k(cp+d)}{cK/2}} \\ &= \sum_{d=0}^{c-1} e^{\frac{-j2\pi kd}{cK/2}} \underbrace{\sum_{p=0}^{K/2-1}\left[\sum_{\tilde{i}=0}^{\tilde{L}-1} e^{\frac{-j2\pi bk\tilde{i}}{c}}\dot{r}_l[cp+d]\right]e^{\frac{-j2\pi kp}{K/2}}}_{FFT}.\end{aligned} \tag{17}$$

For the odd signal component, the received samples $\{r[n]\}$ are demodulated as

$$\begin{aligned}\hat{a}_{l,2k+1} &= \sum_{n=0}^{L_g-1} r[n+(l+\tfrac{1}{2})\tau N]g^*[n]e^{-j2\pi(2k+1)\frac{\upsilon n}{K}} \\ &= \sum_{n=0}^{L_g-1} \tilde{r}_l[n]e^{-j2\pi(2k+1)\frac{\upsilon n}{K}}\end{aligned} \tag{18}$$

where $\tilde{r}_l[n] = r[n+(l+\frac{1}{2})\tau N]g^*[n]$. Following (15)-(17), (18) becomes (19) at the bottom of this page and the steps (a) and (b) in (19) are the same as in (16) and (17). Hence, for the even or odd component, after windowing with the shaping pulse, the demodulation can be effectively implemented by c parallel $K/2$-point FFT blocks whose outputs are combined with proper phase rotations before the summation operation. The block diagram of the demodulator is shown in Fig. 1(b).

C. Complexity Analysis

For the sake of simplicity, we will mainly focus on the complexity of the proposed modulator in one symbol period. In conventional implementation schemes described by [5], the complexity is dominated by the pulse shaping employed in each subcarrier. Hence, the complexity is $\mathcal{O}(KL_g)$. In the proposed scheme, the complexity is dominated by c parallel $K/2$-point IFFT blocks both for the even and odd components followed by the corresponding pulse shaping operations. The overall complexity of the modulator is thus $\mathcal{O}(cK\log_2(K/2)+2L_g)$. Hence, the computational complexity can be greatly reduced by the proposed scheme. For example, the complexity of the proposed scheme with $K = 128$ subcarriers, frequency packing factor $\upsilon = 3/4$, i.e., $b = 3, c = 4$, and pulse length $L_g = 6N, N = K$, can be reduced as much as 21 times than the conventional scheme.

$$\begin{aligned}\hat{a}_{l,2k+1} &= \sum_{n=0}^{K/2-1}\sum_{\tilde{i}=0}^{\tilde{L}-1} \tilde{r}_l[n+\tilde{i}K/2]e^{-j\pi(2k+1)b\tilde{i}/c}e^{-j2\pi(2k+1)bn/cK} \overset{(a)}{=} \sum_{\ddot{n}=0}^{cK/2-1}\sum_{\tilde{i}=0}^{\tilde{L}-1} e^{-j\pi(2k+1)b\tilde{i}/c}\ddot{r}_l[\ddot{n}]e^{-j2\pi(2k+1)\frac{\ddot{n}}{cK}} \\ &\overset{(b)}{=} \sum_{d=0}^{c-1}\sum_{p=0}^{K/2-1}\sum_{\tilde{i}=0}^{\tilde{L}-1} e^{-j\pi(2k+1)b\tilde{i}/c}\ddot{r}_l[cp+d]e^{-j2\pi(2k+1)(cp+d)/cK} \\ &= \sum_{d=0}^{c-1} e^{\frac{-j2\pi(2k+1)d}{cK}} \underbrace{\sum_{p=0}^{K/2-1}\left[\sum_{\tilde{i}=0}^{\tilde{L}-1} e^{\frac{-j\pi(2k+1)b\tilde{i}}{c}}\ddot{r}_l[cp+d]\right]e^{\frac{-j2\pi p}{K}}e^{\frac{-j2\pi kp}{K/2}}}_{FFT}\end{aligned} \tag{19}$$

This article has been accepted for publication in a future issue of this journal, but has not been fully edited. Content may change prior to final publication. Citation information: DOI 10.1109/LCOMM.2017.2774260, IEEE Communications Letters

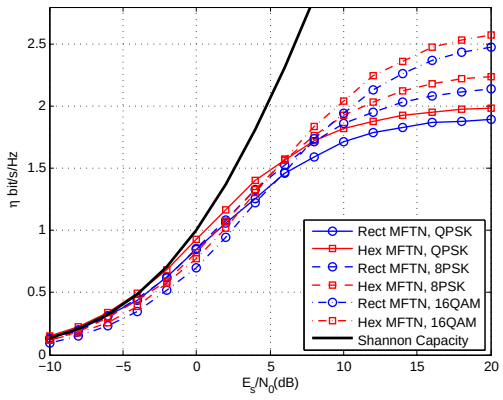

Fig. 2. ASE of rectangular and hexagonal MFTN with different modulation formats.

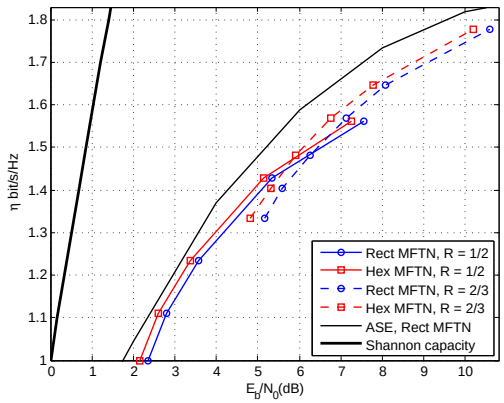

Fig. 3. Spectral efficiency versus required SNR for rectangular and hexagonal MFTN signaling systems. In this figure, the modulation format is QPSK.

IV. System Performance

Based on the channel model (5), we will now evaluate the achievable spectral efficiency (ASE) for MFTN signaling system. More details about the calculation of the ASE can be found in [2], [12]. In the simulations, $K = 80$, $L_g = 6N$, and the Gaussian pulse as [4], [6] with the same standard deviation in time and frequency is employed.

Fig. 2 shows the ASE as a function of the SNR for MFTN and optimized time-frequency spacing values—the values of $T_\Delta = \tau T$ and $F_\Delta = \upsilon F$ are obtained by a coarse search followed by interpolation of the obtained values (fine search).[1] Moreover, a few M-ary phase shift keying (M-PSK) or quadrature amplitude modulation (M-QAM) formats have been considered, namely quaternary ($M = 4$) PSK (QPSK), 8PSK and 16QAM. It can be observed from the figure that the lattice staggered MFTN systems own a better spectral efficiency performance than conventional rectangular MFTN signaling systems. Also, these information-theoretic results can be approached by using proper coding schemes. As an example, we simulated the bit-error-rate (BER) of these two MFTN signaling systems using QPSK modulation, and employing the rate $R = 1/2$ and $2/3$ LDPC codes having code words of 64800 bits of the DVB-S2 standard and with 25 inner iterations. Assuming a reference for the BER of 10^{-5}, the performance of these two systems has been reported in Fig. 3. As a reference, the ASE of conventional rectangular MFTN signaling system is also presented. It can be observed that despite the lack of an optimization in the code design, we have a loss of less than 1dB from the theoretical results.[2]

V. Conclusion

In this letter, we investigated lattice staggered MFTN, where the optimal hexagonal lattice over IPI channels has been considered. For an efficient system implementation involving frequency packing, the low complexity IFFT/FFT-based modulator and demodulator have been proposed, and which substantially reduced the computational complexity than conventional implementation scheme. The practical spectral efficiency and error performance evaluation further validated that the lattice staggered MFTN has a better system performance than conventional rectangular MFTN signaling schemes.

[1]We remark that since we mainly consider finite number of subcarriers K and length of the shaping pulse L_g, the ASE obtained here is slightly worse than that of [12]. However, if L_g is long enough and with infinite transmission in both the time and frequency domains, the ASE will approach [12].

[2]It should be noted that the Shannon capacity could be further approached by using more sophisticated detection schemes, such as the MAP equalization or iterative turbo equalization as given in [2], [5] and [9]. However, this is often at the price of substantially increased complexity at the receiver.

References

[1] P. Banelli, S. Buzzi, G. Colavolpe, et al, "Modulation formats and waveforms for 5G networks: Who will be the heir of OFDM?" *IEEE Signal. Process. Mag.*, vol. 31, no. 6, pp. 80-93, Jul. 2014.

[2] A. Piemontese, A. Modenini, G. Colavolpe and N. S. Alagha, "Improving the spectral efficiency of nonlinear satellite systems through time-frequnecy packing and advanced receiver processing," *IEEE Trans. Commun.*, vol. 61, no. 8, pp. 3404-3412, Aug. 2013.

[3] G. Colavolpe and T. Foggi, "Time-frequency packing for high-capacity coherent optical links," *IEEE Trans. Commun.*, vol, 62, no. 8, pp. 2986-2995, Aug. 2014.

[4] T. Strohmer and S. Beaver, "Optimal OFDM design for time-frequency dispersive channels," *IEEE Trans. Commum.*, vol. 51, no. 7, pp. 1111-1122, Jul. 2003.

[5] F. Rusek, J. B. Anderson, "Multistream faster than Nyquist signaling," *IEEE Trans. Commun.*, vol. 57, no. 5, pp. 1329-1340, May. 2009.

[6] S. Peng, A. Liu, X. Pan and H. Wang, "Hexagonal multicarrier faster-than-Nyquist signaling," *IEEE Access*, vol. 5, pp. 3332-3339, Mar. 2017.

[7] N. Moret and A. M. Tonello, "Design of orthogonal filtered multitone modulation systems and comparison among efficient realizations,", *EURASIP J. Advan. Signal Process.*, vol. 2010, 1-18, 2010.

[8] A. Sahin, I. Guvenc and H. Arslan, "A survey on multicarrier communications: Prototype filters, lattice structures, and implementation aspects," *IEEE Commun Surv & Tutorial.*, vol. 16, no. 3, pp. 1312-1338, Third Quarter. 2014.

[9] D. Dasalukunte, F. Rusek and V. Owall, "Multicarrier faster-than-Nyquist transceivers: Hardware architecture and performance analysis," *IEEE Trans. Circuits. Syst. I, Reg. Papers*, vol. 58, no. 4, pp. 827-836, Apr. 2011.

[10] A. Marquet, D. Roque, C. Siclet and P. Siohan, "FTN multicarrier transmission based on tight Gabor frames," *EURASIP J. Wireless Commun & Network.*, vol. 97, no. 1, pp. 1-15, 2017.

[11] S. Peng, A. Liu, X. Tong and K. Wang, "On max-SIR time-frequency packing for multicarrier faster-than-Nyquist signaling," *IEEE Commun. Lett.*, vol. 21, no. 10, pp. 2142-2145, Oct. 2017.

[12] A. Barbieri, D. Fertonani and G. Colavolpe, "Time-frequency packing for linear modulations: Spectral efficiency and practical detection schemes," *IEEE Trans. Commun.*, vol. 57, no. 10, pp. 2951-2959, Oct. 2009.

[13] G. Matz, D. Schafhuber, K. Grochenig, et al, "Analysis, optimization, and implementation of low-interference wireless multicarrier systems", *IEEE Trans. Wireless. Commun*, vol. 5, no. 6, pp. 1921-1931, May. 2007.